Analyst

COMMUNICATION

View Article Online
View Journal

Cite this: DOI: 10.1039/c6an00793g

Received 5th April 2016,
Accepted 28th May 2016

DOI: 10.1039/c6an00793g

www.rsc.org/analyst

Graphene oxide-based electrochemical label-free detection of glycoproteins down to aM level using a lectin biosensor†

L. Klukova,[a] J. Filip,[b] S. Belicky,[a] A. Vikartovska[a] and J. Tkac*[a]

A label-free ultrasensitive impedimetric biosensor with lectin immobilised on graphene oxide (GO) for the detection of glycoproteins from 1 aM is shown here. This is the first time a functional lectin biosensor with lectin directly immobilised on a graphene-based interface without any polymer modifier has been described. The study also shows that hydrophilic oxidative debris present on GO has a beneficial effect on the sensitivity of (8.46 ± 0.20)% per decade for the lectin biosensor compared to the sensitivity of (4.52 ± 0.23)% per decade for the lectin biosensor built up from GO with the oxidative debris washed out.

Introduction

Saccharides are the most ubiquitous organic molecules in nature and, along with proteins, lipids and nucleic acids, form all living systems.[1] Therefore, it is not surprising that glycans (complex saccharides formed by monosaccharides connected *via* glycosidic bonds) play a crucial role in various vital processes.[2–4] Moreover, in comparison to proteins or DNA, glycans are better equipped to be an information coding tool, because information can be effectively stored by the large variability in saccharidic building blocks that are put together to form glycans.[5]

Furthermore, glycans play a crucial role in the aetiology of all human diseases.[6–8] Glycans are often attached to proteins (more than 70% of human proteins are glycosylated) or lipids and thus glycans are present on cell surfaces at every level of life and create a "sweet" coat reflecting the physiological state of the individual cell.[9] It has been proven that changes in glycosylation patterns of proteins are closely related to the origin and development of various types of cancer or autoimmune disorders.[10] Consequently, the majority of already approved cancer biomarkers are glycoproteins.[11] This means that monitoring of aberrant glycosylation can distinguish healthy individuals from sick patients and has a great potential to be successfully applied in early-stage diagnostics.[12]

The current trend in modern diagnostics is toward simplicity, speed and cost-effectiveness of analyses, with a possibility of point-of-care testing. However, it is quite challenging to meet all the requirements mentioned above. Traditional analytical methods often require complex instrumentation or labelling of molecules, which makes the whole process time and reagent consuming.[13] Contrary to this, electrochemical and other methods, including quartz crystal microbalance, electrochemical impedance spectroscopy (EIS), cyclic voltamperometry or field-effect transistor (FET) based sensing, provide a very smart way to overcome some of the drawbacks of instrumental-based approaches.[12,14]

Nowadays, there is an expansion of electrochemical platforms utilizing graphene and graphene-based materials, which improve the sensing performance of biosensors.[15–19] Since 2004[20] these novel materials have attracted worldwide attention thanks to their impressive properties, especially their high sensing area and conductivity.[21–23] Moreover, graphene oxide (GO) prepared by Hummers' method[24] is commercially available at low cost and due to the richness of its functional groups it can be easily functionalised.[25–29] Several research groups have demonstrated that GO contains a complex mixture of highly oxidized polyaromatic carboxylated fragments (oxidative debris – OD, discovered in 2011 by Wilson's group)[30] which can significantly tune the interfacial behaviour of graphene materials.[31,32] All of these attributes make graphene-based materials suitable for electrochemical biosensing.[33–35]

There are some bioassays reported which combine lectins (carbohydrate binding proteins)[36] and graphene material. Most of them, however, employ lectins as a probe for immobilisation/adsorption of antibodies,[37] cells[38,39] or enzymes,[40] instead of direct biorecognition of glycoproteins. Recently, it was described that the ability of Concanavalin A (Con A) immobilised on pure graphene to bind its analyte was strongly negatively affected, compared to Con A immobilised on gra-

[a]*Department of Glycobiotechnology, Institute of Chemistry, Slovak Academy of Sciences, Dubravska cesta 9, 845 38 Bratislava, Slovakia. E-mail: Jan.Tkac@savba.sk*
[b]*Centre for Advanced Materials, Qatar University, P.O. Box 2713, Doha, Qatar*
†Electronic supplementary information (ESI) available. See DOI: 10.1039/c6an00793g

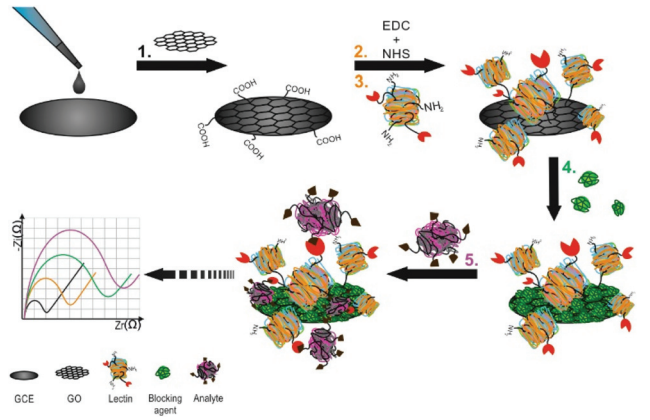

Scheme 1 A scheme showing several modification steps needed for the construction of an impedimetric lectin biosensor involving: 1. modification of the glassy carbon electrode by GO; 2. activation of –COOH groups present on the surface by EDC/NHS; 3. covalent immobilisation of Con A lectin; 4. blocking of the interface by a carbo-free blocking agent. Step 5 is incubation of the biosensor with its analyte.

phene covered by a self-assembled layer.[41] This suggests strong adsorption of Con A onto a hydrophobic graphene surface, negatively influencing the structural integrity of Con A. This is why in the current work we wanted to show that an increased hydrophilicity of graphenic material can have a beneficial role on the binding ability of immobilised Con A. In order to prove this hypothesis, two different graphenic materials were tested as a support for the immobilisation of Con A: a highly hydrophilic GO and base-washed GO (GObw) with a moderate hydrophobicity achieved by the removal of highly hydrophilic oxidative debris from the surface of GO. Finally, by the careful building of an interface based on GO with immobilised lectin, an ultrasensitive detection of glycoproteins could be achieved, observed previously only on modified gold electrodes.[42,43] Here we show for the first time that glycoproteins could be detected with EIS applied as a transducing platform down to attomolar concentration using lectins directly immobilised on a GO modified interface (Scheme 1).

Results and discussion

UV-Vis characterisation of GO and GObw

The first experiment performed either with GO or GObw was the investigation of the UV-Vis properties of a commercially available GO solution and a GObw aqueous solution prepared from lyophilised powder. The results indicate that the GO solution exhibits two maxima, at 230 nm (due to π–π transitions of the aromatic C=C bond) and at 300 nm (due to n–π transitions of the C=O bond) (Fig. S1a†) in agreement with data in the literature,[39] while GObw exhibited only one maximum at 256 nm (Fig. S2a†).

Calibration curves, *i.e.* absorbance peak heights *vs.* sample concentration, could also be applied to extract extinction coefficients for both types of sample. A calibration curve for GO (Fig. S1b†) is a straight line with R^2 = 0.978 and an extinction coefficient of (0.0986 ± 0.0067) ml μg^{-1} cm^{-1}, while a calibration curve for GObw (Fig. S2b†) is a perfectly straight line with R^2 = 0.999 and an extinction coefficient of (0.0190 ± 0.0001) ml μg^{-1} cm^{-1}, suggesting that GObw is an optically less dense material than GO. Such characterisations of GO and GObw allowed us to work with the same concentration of both materials (GO and GObw) in the subsequent experiments.

FTIR and Raman characterisation of GO and GObw

Fourier transform infrared (FTIR) experiments (Fig. S3a†) revealed the presence of a broad peak from 2800 to 3800 cm^{-1} for GO, attributable to ν(C–OH, COOH, H_2O) and several sharp peaks between 1000 and 1800 cm^{-1}. A peak appearing at 1630 cm^{-1} previously assigned to in-plane vibrations of an sp^2-hybridised C–C bond[30] is present in the GO sample with a mild shift to 1580 cm^{-1} for the GObw sample. Peaks appearing for GO could be assigned to ν(C–O–C) at 1076 cm^{-1}, to ν(C–OH) at 1258 cm^{-1}, to ν(carboxy C–O) at 1411 cm^{-1} and to ν(C=O) at 1723 cm^{-1}, in agreement with data in the literature.[40,44] Peaks for GObw could be assigned to ν(C–OH) at 1239 cm^{-1} and to ν(C=O) at 1718 cm^{-1}, suggesting that a certain amount of oxygen-containing moieties resisted the harsh conditions during base washing. Their diversity, however, was significantly decreased.

The quality of graphene-based samples is often studied by analysis of the D-band peak at around 1300 cm^{-1} (due to breathing modes in C–C structures indicating defects) and of the G-band peak at 1600 cm^{-1} (due to C(sp^2)–C(sp^2) bond stretching vibrations).[30] Raman experiments (Fig. S3b†) showed peaks for GO at 1349 cm^{-1} and 1600 cm^{-1}, in agreement with the literature[30,45] and for the GObw sample slightly changed positions of the peaks at 1339 cm^{-1} and 1605 cm^{-1} were observed, again in agreement with data in the literature for base-washed GO.[30] Base washing of GO did not result in a change in the D/G ratio, with a value of 0.995 for GO and 1.011 for GObw, in agreement with the literature.[30] This confirms that base washing only displaced OD from the GO surface, without reduction of GO.

AFM measurements

Atomic force microscopy (AFM) was applied to look at the interfacial features during the build-up of the lectin biosensor, involving subsequent modifications of the interface (Fig. 1a) by GO (Fig. 1b), Con A (Fig. 1c), a blocking agent (Fig. 1d), and with a final incubation of the interface with analyte invertase (INV) (Fig. 1e).

Typical features to be seen on the interface during modification of the planar surface are shown in Fig. 1f. The mean square surface roughness (R_q) of the bare interface decreased from 0.36 nm to 0.12 nm upon incubation with a GO solution and the surface was covered with flat GO sheets, but some small features were visible (Fig. 1b). After covalent immobilisation of Con A lectin on a GO modified interface using a standard amine coupling (*i.e.* EDC/NHS coupling chemistry), the roughness of the interface increased sharply with

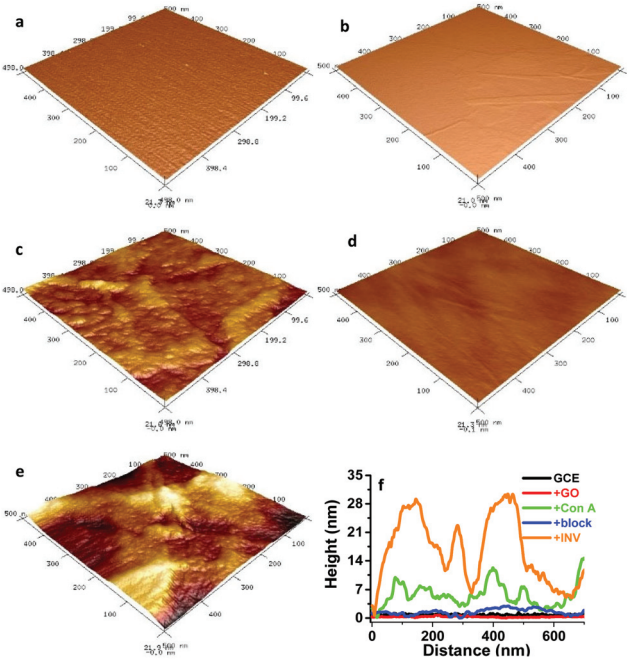

Fig. 1 Atomic force microscopy (AFM) of (a) a bare surface, (b) a GO-modified interface, (c) the surface with covalently immobilised Con A, (d) the interface blocked with a carbo-free blocking solution, (e) the surface after incubation with its analyte invertase (INV) and (f) a topographical profile of surfaces depicted in (a–e).

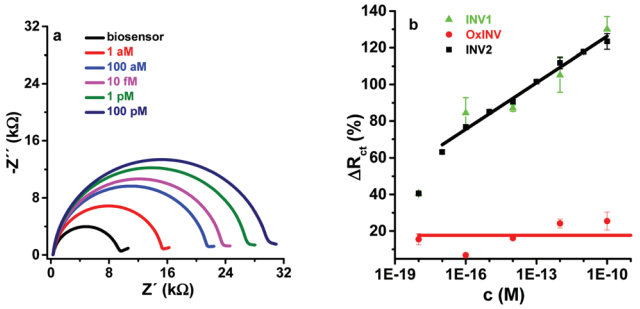

Fig. 2 (a) Nyquist plots after incubation of the Con A lectin biosensor with INV as an analyte in a concentration window from 1 aM to 100 pM and (b) two independent calibration curves of the Con A lectin biosensor towards an analyte INV (INV1 and INV2) and a negative control, which was an oxidised form of INV (oxINV).

R_q = 2.62 nm, with a possibility of seeing individual Con A proteins on the surface (Fig. 1c and f, green line). The features with heights around or below 10 nm seen on the surface after immobilisation of Con A are consistent with the molecular size of intact Con A (6.7 × 11.3 × 12.2 nm) being a tetramer with M_w = 104 kDa, while Con A on the surface can also dissociate into dimers (6.1 × 8.6 × 9.1 nm) or monomers (4.2 × 4.0 × 3.9 nm).[42] In the next step the surface was blocked by a carbo-free blocking agent to prepare an interface resistant to non-specific interactions, and the surface roughness again decreased to an R_q value of 0.73 nm. When the surface was incubated with an analyte, *i.e.* INV, the surface roughness sharply increased to an R_q value of 6.86 nm. INV is a much larger protein with M_w = 270 kDa compared to Con A, and it can form oligomers as shown recently,[46] and thus it is not surprising to see much larger features after interaction of the surface with INV (Fig. 1f, brown line) compared to the presence of Con A on the surface (Fig. 1f, green line).

Biosensor development

Two different Con A biosensors based on either GO or GObw were prepared, but the biosensor based on GObw was less sensitive towards its analyte (INV), with a sensitivity of (4.52 ± 0.23)% per decade, while the biosensor based on GO offered a sensitivity of (8.46 ± 0.20)% per decade (R^2 = 0.996 for INV2, Fig. 2b). Moreover, the lectin biosensor based on GO offered highly reproducible detection of its analyte INV, with RSD in the range from 0.2% to 3.5% with an average RSD of 1.6%. The lower sensitivity of the lectin biosensor based on GObw could be due to the increased hydrophobicity of GObw compared to GO by the removal of highly oxidised OD. Recently it was shown that the binding ability of Con A immobilised on pure graphene was severely affected, with a 12-fold decrease of Con A's binding ability compared to Con A immobilised on graphene covered by a self-assembled layer.[41] The Con A biosensor based on GO offers a linear working range spanning at least 7 orders of magnitude from a concentration of 10 aM up to 100 pM (curve INV2, Fig. 2b). Two independent calibration curves (INV1 and INV2) with the biosensor devices prepared on different days are shown in Fig. 2b, indicating high reliability of biosensor preparation as judged from similar sensitivities: (8.46 ± 0.20)% per decade (INV2) and (9.13 ± 2.19)% per decade (INV1 with RSD in the range from 0.7% to 9.9% with an average RSD of 5.4%). Quite interestingly, when oxidised INV (oxINV) was incubated with the biosensor, a low and stable response in the whole concentration window investigated was observed, suggesting a low non-specific protein binding.

The equilibrium dissociation constants K_{Dsurf} of the lectin biosensor with immobilised Con A towards its analyte (INV) and a non-specific binding probe (oxINV) were evaluated using a non-linear fitting of linear calibration curves (*i.e.* $\Delta R_{ct} = f(c)$) for both proteins using a Hill1 model employing OriginPro9.1 software with a number of cooperative sites fixed (n = 1). As shown in Fig. S4,† the equilibrium dissociation constant for INV was evaluated as K_{Dsurf} = (9.3 ± 4.4) aM with R^2 = 0.988 and for oxINV as K_{Dsurf} = (9.1 ± 6.0) fM with R^2 = 0.916. This means that the affinity of the immobilised Con A for INV is 3 orders of magnitude stronger compared to oxINV and that oxINV can be considered to be a reliable non-specific binding probe. Typical Nyquist plots showing the EIS response of the biosensor towards its analyte INV are shown in Fig. 2a.

The impedimetric lectin biosensor presented here is among the most sensitive electrochemical biosensor devices described so far,[12,14] with a detection limit better than or comparable to electrochemical lectin-based detection platforms developed on modified gold electrodes with tuned interfacial properties.[42,43,47]

Bioanalytical approaches based on the integration of lectins and graphene or GO have been described in the literature, but have not been applied to the detection of glycoproteins in a label-free format of analysis with Con A directly immobilised on graphene or GO. For example, GO or reduced GO patterned by glycans/carbohydrates has been employed for the detection of lectins (including Con A) using electrochemical,[45,48] electric[49] and electrochemiluminiscent[50,51] detection platforms. Con A linked to graphene or GO *via* glycans or polymers has been employed for the immobilisation of antibodies to the electrode surface for electrochemical immunosensing of various analytes including cancer biomarkers[37,52,53] or for enzyme-less electrochemical detection of glucose.[54,55]

The most similar concepts to ours were described recently of Con A immobilised on graphene or reduced GO using an organic linker, but involving labels in a sandwich configuration.[38,56] Thus, the approach we have developed is the first to describe the direct immobilisation of Con A on a graphenic material (GO) for label-free detection of glycoproteins.

Finally, two serum samples (with details provided in the ESI† file) diluted 1000 times – one from a healthy individual and the other one from a patient with rheumatoid arthritis (RA) were analysed by the impedimetric lectin biosensor. The results showed that the biosensor response was larger: (154 ± 14)% for the RA patient compared to the response of (68 ± 9)% observed for the healthy individual. This observation is in good agreement with our previous results, showing a larger response of the biosensor in the case of the sample from the RA patient compared to analysis of a serum sample from a healthy individual.[42]

Conclusions

The study shows the importance of oxidation debris present on GO surface to keep immobilised Con A lectin functional for bioaffinity interactions with its analyte. Moreover, when oxidation debris is present on GO, the high density of oxygen-containing functional groups could be effectively employed for covalent immobilisation of the lectin. Thus, here we have shown for the first time that Con A immobilised to GO without any polymer modifier could be used for ultrasensitive detection of glycoproteins from an aM concentration range. Furthermore, since EIS was employed as a transducing platform, label-free detection was possible, offering a wide working concentration window for glycoprotein analysis. This study is a solid foundation for others, suggesting that a direct immobilisation of biorecognition elements to graphenic interfaces is feasible, but adsorption of the biorecognition elements to hydrophobic graphenic surfaces should be avoided to keep the biointerface functional as described recently.[41] This has to be taken into account, especially for biorecognition of elements that have only one binding site, since the denaturation of such binding elements could affect their binding ability to a higher extent than Con A containing four binding sites.

Acknowledgements

Funding from the Slovak research and development agency APVV-14-0753 and VEGA 2/0162/14 is acknowledged. This report was made possible by a NPRP award [NPRP grant no. 6-381-1-078] from the Qatar National Research Fund (a member of The Qatar Foundation). The research leading to these results has received funding from the European Research Council under the European Union's Seventh Framework Program (FP/2007-2013)/ERC Grant agreement no. 311532 and from the European Union's Seventh Framework Programme for research, technological development and demonstration under grant agreement no. 317420. This publication is the result of the project implementation: Centre for materials, layers and systems for applications and chemical processes under extreme conditions – Stage I, ITMS no. 26240120007 supported by the Research & Development Operational Program funded by the ERDF.

References

1 E. Maverakis, K. Kim, M. Shimoda, M. E. Gershwin, F. Patel, R. Wilken, S. Raychaudhuri, L. R. Ruhaak and C. B. Lebrilla, *J. Autoimmun.*, 2015, **57**, 1–13.
2 A. Helenius and M. Aebi, *Science*, 2001, **291**, 2364–2369.
3 K. Ohtsubo and J. D. Marth, *Cell*, 2006, **126**, 855–867.
4 G. A. Rabinovich and M. A. Toscano, *Nat. Rev. Immunol.*, 2009, **9**, 338–352.
5 S. Belicky and J. Tkac, *Chem. Pap.*, 2015, **69**, 90.
6 R. Moon, *Transforming Glycoscience: A Roadmap for the Future*, The National Academies Press, Washington, D.C., 2012.
7 M. M. Fuster and J. D. Esko, *Nat. Rev. Cancer*, 2005, **5**, 526–542.
8 A. Varki, *Nature*, 2007, **446**, 1023–1029.
9 R. D. Cummings and J. M. Pierce, *Chem. Biol.*, 2014, **21**, 1–15.
10 D. H. Dube and C. R. Bertozzi, *Nat. Rev. Drug Discovery*, 2005, **4**, 477–488.
11 S. A. Svarovsky and L. Joshi, *Anal. Methods*, 2014, **6**, 3918–3936.
12 L. Klukova, T. Bertok, P. Kasak and J. Tkac, *Anal. Methods*, 2014, **6**, 4922–4931.
13 W. R. Alley Jr., B. F. Mann and M. V. Novotny, *Chem. Rev.*, 2013, **113**, 2668–2732.
14 E. Paleček, J. Tkáč, M. Bartošík, T. Bertók, V. Ostatná and J. Paleček, *Chem. Rev.*, 2015, **115**, 2045–2108.
15 D. Chen, H. Feng and J. Li, *Chem. Rev.*, 2012, **112**, 6027–6053.
16 D. A. C. Brownson, D. K. Kampouris and C. E. Banks, *Chem. Soc. Rev.*, 2012, **41**, 6944–6976.
17 Y. Liu, X. Dong and P. Chen, *Chem. Soc. Rev.*, 2012, **41**, 2283–2307.
18 M. Pumera, *Chem. Soc. Rev.*, 2010, **39**, 4146–4157.

19 G. Yang, C. Zhu, D. Du, J. Zhu and Y. Lin, *Nanoscale*, 2015, **7**, 14217–14231.
20 K. S. Novoselov, A. K. Geim, S. V. Morozov, D. Jiang, Y. Zhang, S. V. Dubonos, I. V. Grigorieva and A. A. Firsov, *Science*, 2004, **306**, 666–669.
21 H. Gao and H. Duan, *Biosens. Bioelectron.*, 2015, **65**, 404–419.
22 K. S. Novoselov, V. I. Fal'ko, L. Colombo, P. R. Gellert, M. G. Schwab and K. Kim, *Nature*, 2012, **490**, 192–200.
23 A. K. Geim, *Science*, 2009, **324**, 1530–1534.
24 W. S. Hummers and R. E. Offeman, *J. Am. Chem. Soc.*, 1958, **80**, 1339–1339.
25 V. Georgakilas, M. Otyepka, A. B. Bourlinos, V. Chandra, N. Kim, K. C. Kemp, P. Hobza, R. Zboril and K. S. Kim, *Chem. Rev.*, 2012, **112**, 6156–6214.
26 C. Chung, Y.-K. Kim, D. Shin, S.-R. Ryoo, B. H. Hong and D.-H. Min, *Acc. Chem. Res.*, 2013, **46**, 2211–2224.
27 C. K. Chua and M. Pumera, *Chem. Soc. Rev.*, 2014, **43**, 291–312.
28 Q. Tang, Z. Zhou and Z. Chen, *Nanoscale*, 2013, **5**, 4541–4583.
29 K. P. Loh, Q. Bao, G. Eda and M. Chhowalla, *Nat. Chem.*, 2010, **2**, 1015–1024.
30 J. P. Rourke, P. A. Pandey, J. J. Moore, M. Bates, I. A. Kinloch, R. J. Young and N. R. Wilson, *Angew. Chem., Int. Ed.*, 2011, **50**, 3173–3177.
31 A. Bonanni, A. Ambrosi, C. K. Chua and M. Pumera, *ACS Nano*, 2014, **8**, 4197–4204.
32 V. R. Coluci, D. S. T. Martinez, J. G. Honório, A. F. de Faria, D. A. Morales, M. S. Skaf, O. L. Alves and G. A. Umbuzeiro, *J. Phys. Chem. C*, 2014, **118**, 2187–2193.
33 J. Liu, X. Leng, Y. Xiao, C. Hu and L. Fu, *Nanoscale*, 2015, **7**, 11922–11927.
34 J. Guo, T. Zhang, C. Hu and L. Fu, *Nanoscale*, 2015, **7**, 1290–1295.
35 L. Bai, Y. Chai, X. Pu and R. Yuan, *Nanoscale*, 2014, **6**, 2902–2908.
36 D. Pihíková, P. Kasák and J. Tkac, *Open Chem.*, 2015, **13**, 636.
37 J. Liu, J. Wang, T. Wang, D. Li, F. Xi, J. Wang and E. Wang, *Biosens. Bioelectron.*, 2015, **65**, 281–286.
38 X. Chen, Y. Wang, Y. Zhang, Z. Chen, Y. Liu, Z. Li and J. Li, *Anal. Chem.*, 2014, **86**, 4278–4286.
39 J. Liu, X. Xin, H. Zhou and S. Zhang, *Chem. – Eur. J.*, 2015, **21**, 1908–1914.
40 X. Zhong, R. Yuan and Y.-Q. Chai, *Sens. Actuators, B*, 2012, **162**, 334–340.
41 T. Alava, J. A. Mann, C. Théodore, J. J. Benitez, W. R. Dichtel, J. M. Parpia and H. G. Craighead, *Anal. Chem.*, 2013, **85**, 2754–2759.
42 T. Bertok, L. Klukova, A. Sediva, P. Kasák, V. Semak, M. Micusik, M. Omastova, L. Chovanová, M. Vlček, R. Imrich, A. Vikartovska and J. Tkac, *Anal. Chem.*, 2013, **85**, 7324–7332.
43 L. Klukova, T. Bertok, M. Petrikova, A. Sediva, D. Mislovicova, J. Katrlik, A. Vikartovska, J. Filip, P. Kasak, A. Andicsova-Eckstein, J. Mosnacek, J. Lukac, J. Rovensky, R. Imrich and J. Tkac, *Anal. Chim. Acta*, 2015, **853**, 555–562.
44 X. Liu, X. Ou, Q. Lu, S. Chen and S. Wei, *Microchim. Acta*, 2015, **182**, 797–803.
45 Z. Li, S.-S. Deng, Y. Zang, Z. Gu, X.-P. He, G.-R. Chen, K. Chen, T. D. James, J. Li and Y.-T. Long, *Sci. Rep.*, 2013, **3**, 2293.
46 M. A. Sainz-Polo, M. Ramírez-Escudero, A. Lafraya, B. González, J. Marín-Navarro, J. Polaina and J. Sanz-Aparicio, *J. Biol. Chem.*, 2013, **288**, 9755–9766.
47 T. Bertok, A. Šedivá, J. Filip, M. Ilcikova, P. Kasak, D. Velic, E. Jane, M. Mravcová, J. Rovenský, P. Kunzo, P. Lobotka, V. Šmatko, A. Vikartovská and J. Tkac, *Langmuir*, 2015, **31**, 7148–7157.
48 X.-P. He, B.-W. Zhu, Y. Zang, J. Li, G.-R. Chen, H. Tian and Y.-T. Long, *Chem. Sci.*, 2015, **6**, 1996–2001.
49 Y. Chen, H. Vedala, G. P. Kotchey, A. Audfray, S. Cecioni, A. Imberty, S. Vidal and A. Star, *ACS Nano*, 2012, **6**, 760–770.
50 J. Zhang, Y. Ruo, S. Chen, X. Zhong and X. Wu, *RSC Adv.*, 2014, **4**, 48465–48471.
51 X. Ou, X. Tan, X. Liu, Q. Lu, S. Chen and S. Wei, *Biosens. Bioelectron.*, 2015, **70**, 89–97.
52 D. Tang, B. Zhang, J. Tang, L. Hou and G. Chen, *Anal. Chem.*, 2013, **85**, 6958–6966.
53 Q. Cong, H. Bian, Z. Yu, J. Liu and F. Xi, *Anal. Methods*, 2015, **7**, 9655–9662.
54 Y. Song, H. Liu, H. Tan, F. Xu, J. Jia, L. Zhang, Z. Li and L. Wang, *Anal. Chem.*, 2014, **86**, 1980–1987.
55 J. Huang, L. Zhang, R.-P. Liang and J.-D. Qiu, *Biosens. Bioelectron.*, 2013, **41**, 430–435.
56 H. Zhou, Y. Yang, C. Li, B. Yu and S. Zhang, *Chem. – Eur. J.*, 2014, **20**, 14736–14743.